Desalination and Water Treatment
www.deswater.com

doi: 10.1080/19443994.2016.1156584

57 (2016) 25435–25449
November

Taylor & Francis
Taylor & Francis Group

Activated carbon selection for the adsorption of marine DOC and analysis of DOC fractionation

Mathias Monnot[a,b,c], Stéphanie Laborie[a,b,c,*], Corinne Cabassud[a,b,c]

[a]*Université de Toulouse; INSA, UPS, INP; LISBP, Hall de Recherche Génie des Procédés, 135 Avenue de Rangueil, F-31077 Toulouse, France, Tel. +33 561559783; email: mathias.monnot@insa-toulouse.fr (M. Monnot), Tel. +33 561559287; email: stephanie.laborie@insa-toulouse.fr (S. Laborie), Tel. +33 561559773; email: corinne.cabassud@insa-toulouse.fr (C. Cabassud)*
[b]*INRA, UMR792 Ingénierie des Systèmes Biologiques et des Procédés, F-31400 Toulouse, France*
[c]*CNRS, UMR5504, F-31400 Toulouse, France*

Received 19 November 2015; Accepted 5 February 2016

ABSTRACT

Adsorption on granular activated carbon (GAC) and fractionation of marine dissolved organic carbon (DOC) was investigated with the objective of mitigating RO membrane biofouling in the context of a reverse osmosis process for seawater pretreated by ultrafiltration. The behaviours of six commercial GAC compounds were compared. Batch kinetics experiments showed that 80% of DOC in seawater was adsorbed within four hours. Adsorption kinetics fitted the Ho and McKay model well, and isotherms followed the Freundlich model. GAC A and GAC F had the best adsorption capacities. For GAC A, the adsorption mechanism was mainly related to high occupation of the porous volume, whereas for GAC F, the adsorption was mainly related to electrostatic interactions. GAC A was selected for a fixed bed column experiment continuously fed with seawater as GAC F released acidic groups into the feed water. This filtration set-up enabled more than 70% of DOC to be removed from seawater. Moreover, LC-OCD analysis showed that GAC A filtration drastically reduced DOC fractions, including colloidal transparent exopolymer particles (cTEP) by 92% and neutral low molecular weight molecules by 80%, thus reducing the potential for biofouling of the RO membranes.

Keywords: Adsorption; Seawater; Organic matter; TEP removal; GAC; Fixed bed

1. Introduction

Seawater reverse osmosis (SWRO) desalination is an efficient and reliable process for supplying drinking water. RO membranes are currently the leading technology for new installations and the field continues to develop [1]. Efficient RO desalination requires good pretreatment to improve its performance and to increase the life of the RO membrane, which is very sensitive to fouling, especially biological fouling [2]. Researchers report that microorganisms secrete transparent exopolymer particles (TEP) or exopolymer substances that attach to the surface of the membrane and can increase biofouling [3–5]. Additionally, because it is a carbon source and promotes the growth of microorganisms, natural organic matter (NOM) in seawater is a significant factor in RO membrane fouling.

Conventional pretreatments were initially used for RO pretreatment, but are increasingly being replaced

*Corresponding author.

1944-3994/1944-3986 © 2016 Balaban Desalination Publications. All rights reserved.

by ultrafiltration (UF) because of the unpredictable variations in seawater quality. The main advantage of a membrane-based process is that it produces a consistent quality of permeate regardless of the condition of the feed water [6]. Nevertheless, the majority of NOM in seawater is dissolved organic carbon (DOC) [7], which cannot be totally removed by UF, where pore sizes are around 0.01 μm. Some researchers report that UF removes only around 10% of marine DOC [8,9].

Therefore, the work reported here couples activated carbon adsorption, for the removal of NOM, with UF for the removal of particles, bacteria and viruses. The combined process has shown good potential for the removal by both powdered activated carbon (PAC) and granular activated carbon (GAC). DOC removal of at least 70% has been obtained with PAC [8,10] and removal of more than 50% with GAC [11,12].

Adsorption of NOM in freshwater or wastewater is well documented. In these fields, GAC adsorption is mainly intended for the removal of micropollutants and so competitive adsorption of NOM needs to be managed [13] or avoided [14]. Zietzschmann et al. [15] demonstrated that the small size fractions of NOM were the source of the majority of adsorption competition with respect to micropollutants, even with highly microporous activated carbon. Furthermore, in fresh waters, Schreiber et al. [16] and Velten et al. [17] showed that these small size fractions of NOM were preferentially adsorbed on GAC, probably because of better accessibility to the micropores of the GAC.

For application as a pretreatment for seawater, the target function of the adsorption is different: adsorption is focused on specific fractions of NOM. As explained earlier, the targeted NOM obviously includes DOC as it is involved in RO biofouling. More precisely, assimilable organic carbon (AOC) is the fraction of DOC that can be easily degraded and used by aquatic microorganisms for their growth. Jeong et al. [18] demonstrated that the quantity of AOC could be directly correlated to the amount of neutral low molecular weight (LMW) molecules of DOC. Therefore, one of the targeted DOC fractions in seawater is those neutral LMW molecules. The main fraction of TEP, composed of biopolymers and involved in biofouling, is colloidal (cTEP). Consequently, cTEP is also a fraction that would be worthwhile to adsorb. Table 1 presents the characteristic sizes of the different NOM fractions that would be interesting to adsorb, together with their usual concentrations in seawater.

In seawater, the interactions between NOM and GAC take place in a saline solution. Thus, the characterization of marine DOC adsorption on GAC in terms of kinetics and isotherms remains to be explored. Spotte and Adams [22] studied DOC removal kinetics in batch mode with artificial seawater and found that about 80% of DOC was removed by various GACs during the first days of operation. This rate decreased to about 20% or less after 70 days, the decrease being attributed to saturation of the GAC. DOC removal was much higher in the case of a GAC with high specific surface area. The kinetics of how equilibrium was reached within the first few minutes of operation was not studied. Therefore, it remains to be observed whether the kinetics of natural seawater DOC adsorption follows one of the common kinetic models, assuming DOC behaves as a single compound.

There are a few studies on marine DOC adsorption isotherms. The two main adsorption isotherm models are those of Langmuir (based on monolayer assumption and constant sorption energy) and Freundlich (empirical model developed for heterogeneous surfaces). In saline water conditions with synthetic seawater, Duan et al. [23] demonstrated that the adsorption of commercial humic acid fitted the Freundlich isotherm well. They also demonstrated that the presence of metal salts, such as Mg^{2+} or Ca^{2+}, could be involved in the complexation of humic acid functional groups, which could create a stronger electrostatic affinity between humic acids and a negatively charged activated carbon. Moreover, they indicated that high ionic strength may compress the electrical double layer of activated carbon surface and humic acid. This would allow Van der Waals attractive forces to have a beneficial effect on adsorption. In both the cases, adsorption of commercial humic acids was enhanced in seawater. This remains to be observed in natural seawater with real marine DOC.

As previously stated, some studies have demonstrated that GAC filters could be a good pretreatment before RO desalination, reducing DOC concentrations in seawater at lab scale. However, very few papers are available on the characterization of marine DOC adsorption behaviour or on the characterization of DOC fractions (particularly TEP and neutral LMW molecules) removed from natural seawater by a GAC adsorption filter. This information is crucial for selecting the best GAC in such filters.

This work aims to:

(1) study the adsorption interactions between marine DOC and GAC in real saline waters in terms of adsorption kinetics and isotherms. Six commercially available GACs having different properties in terms of material, surface charge, porous volume and specific surface area were chosen for these experiments. Adsorption kinetics and isotherms will be compared and

Table 1
Characteristic size and usual concentration of the targeted marine NOM fractions

	NOM fraction		
	DOC	cTEP	LMW neutrals
Average size or molecular weight [19]	<0.45 μm	>150,000 Da and <0.45 μm	<350 Da
Range of concentration in seawater (mg L^{-1})	1.0–2.0 [20]	0.3–1.5 [21]	0.2–1.5 [18]

discussed in order to select the GAC that has the highest DOC adsorption capacity and uptake rate.

(2) provide a first evaluation of the capacity of a fixed bed containing the selected GAC to remove DOC, TEP and neutral LMW marine organic molecules. Testing will be at a semi-industrial scale, with a continuous feed of seawater and characterization of the feed and filtrated waters.

2. Materials and methods

2.1. Seawater and GACs

Seawater was sampled from the Mediterranean Sea from June 2013 to January 2014, and was found to have an average salinity of 36 g L^{-1} and an average DOC of 1.9 mg L^{-1}. Seawater was stored for less than one month in a mixed, refrigerated tank at a temperature of 4°C in order to prevent biological growth. Table 2 presents the characteristics of this seawater.

Various activated carbons were chosen according to characteristics such as their material, activation mode (physical or chemical), specific surface area and porous volume. The main characteristics of the GAC granules given by the manufacturers are summarized in Table 3. The diameter of the granules was of the same order of magnitude (around 1 mm) for all GAC media so, for the same hydrodynamics, external transport conditions between the GACs should not change. However, specific surface area varied from 950 to 1,800 m^2 g^{-1} and the internal porous networks were very different as the microporous volume/mesoporous volume ratio varied from 0.8 to about 10.

Before use, each GAC medium was washed with a large amount of ultrapure water to remove colloidal fractions, oven-dried at 105°C for at least 24 h, and then kept in a desiccator until use.

2.2. Dissolved organic matter assessment

The total organic carbon (TOC) concentration was measured with a TOC-meter (TOC-VCSH, Shimadzu) using the non-purgeable organic carbon method, which corresponded to the measurement of DOC as particulate organic carbon was removed through 0.45 μm polytetrafluoroethylene (PTFE) syringe filters. The detection limit of the TOC-meter was 0.1 mg L^{-1} TOC in the presence of high salt concentrations, as was the case for seawater.

2.3. UV absorbance at 254 nm

Ultraviolet (UV) absorbance at 254 nm is a property of molecules containing unsaturated carbon atoms, e.g. in the aromatic rings that are constituent parts of humic acids. It was measured using a Jasco UV–vis spectrophotometer (V630) with quartz cuvettes of 1 cm path length.

2.4. LC-OCD-UVD analysis and colloidal transparent exopolymer particles (cTEP) concentration

Liquid chromatography with organic carbon detection (LC-OCD) is a fractionation method based on size exclusion chromatography coupled with two different detectors: an organic carbon detector (OCD) and a UV

Table 2
Properties of the seawater samples

Property	Minimum	Average	Maximum
pH	7.9 ± 0.1	8.0 ± 0.1	8.2 ± 0.1
Turbidity (NTU)	0.65 ± 0.02	2.8 ± 0.1	6.6 ± 0.2
Conductivity (mS cm^{-1})	56.2 ± 0.3	59.0 ± 0.3	62.3 ± 0.3
$UV_{254\ nm}$ absorbance	0.027 ± 0.002	0.036 ± 0.002	0.048 ± 0.002
DOC (mg L^{-1})	1.6 ± 0.1	1.9 ± 0.1	2.3 ± 0.1

Table 3
Characteristics of the GACs selected for this study

Property of GAC	A	B	C	D	E	F
Commercial name	Carbsorb 40	PICA F22	Norit 830 W	PICA S23	PICA S35	PICA L27
Material	Bituminous coal	Bituminous coal	Bituminous coal	Coconut	Coconut	Wood
Activation	Physical	Physical	Physical	Physical	Physical	Chemical
Specific surface BET ($m^2\ g^{-1}$)	950	1,000	1,100	1,250	1,700	1,800
Microporous volume ($cm^3\ g^{-1}$)	0.42	0.38	0.17	0.50	0.64	0.70
Mesoporous volume ($cm^3\ g^{-1}$)	0.15	0.10	0.21	0.05	0.11	0.35
Granule diameter (mm)	0.43–1.7	0.43–1.7	0.6–2.3	1.46[a]	0.5–0.8	0.85–2.0

[a]Only mean diameter was given by manufacturer.

absorbance detector at 254 nm. The measurement procedure has been described in detail by Huber et al. [19]. LC-OCD-UVD enables organic molecules to be separated into five different fractions according to their molecular size: biopolymers composed of polysaccharides and proteins (>20 kDa), humics (and fulvics) (~1 kDa), building blocks that correspond to breakdown products of humics (0.3–0.5 kDa), LMW organic acids and LMW neutrals (alcohols, aldehydes, ketones and amino acids) (<0.3 kDa). In seawater, the two major components are LMW molecules and humic substances [24,25]. Only hydrophilic DOC fractions can be quantified by LC-OCD analysis. Jeong et al. [12] showed that most of the DOC in seawater was hydrophilic and could make up about 60%. LC-OCD also enables quantification of cTEP concentration [19], which is defined as the part of the biopolymers fraction above 150 kDa and below 0.45 μm. cTEP is present at a higher concentration than particulate TEP in seawater [4].

2.5. pH of the point of zero charge

The pH of the point of zero charge pH_{PZC}, i.e. the pH for which the total surface charge of the granule is zero was measured by the drift method [26]. Above this pH, the total surface of the granular medium was negatively charged. For this purpose, 100 mL of a 0.01 M NaCl solution was placed in bottles at a constant room temperature of 21°C and N_2 was bubbled through the solution to stabilize the pH by preventing the dissolution of CO_2. The pH was then adjusted to successive initial values between 3 and 11, by adding either HCl or NaOH, and the GAC (0.5 g) was added to the solution. The final pH, reached after at least 24 h, was measured and plotted as a function of the initial pH. The pH at which the curve crossed the line $pH_{(final)} = pH_{(initial)}$ was the pH_{PZC} of the given carbon as illustrated in Fig. 1.

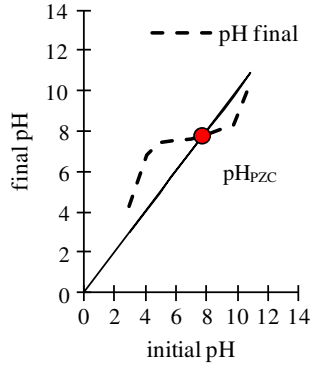

Fig. 1. Graphical resolution to determine pH_{PZC}.

2.6. Kinetic experiments in batch mode

Determination of adsorption kinetics was performed with seawater and for each GAC at room temperature (around 20°C) by adding 14.0 g of GAC into a beaker containing 2 L of seawater and mixing the suspension using an overhead shaker at the maximum speed of 15 rpm for at least 8 h. The maximum speed was chosen to reduce the mass transfer limitation due to external transport. During the kinetic experiment, samples of 20 mL were taken from the beaker after different periods of time and filtered through a 0.45-μm filter before DOC was analysed. The quality of GAC adsorption was evaluated in terms of DOC removal (%), which was estimated from the following equation:

$$R_{DOC} = \frac{(C_i - C_t)}{C_i} \times 100 \quad (1)$$

where C_i and C_t are respectively the initial DOC concentration and DOC concentration at time t.

The correlation with most common kinetic adsorption models was studied according to their linearized

equations presented in Table 4. These models are the following [27]: Lagergren; Ho and McKay; Weber and Morris; and Elovich and Zhabrova. The correlation between the experimental points and models was evaluated by means of the correlation factor R^2.

In table 4, q_t and q_e are the amount adsorbed at time t and at equilibrium (mg g^{-1}), respectively; k_1, k_2 and k_i are the pseudo-first-order rate constant (min^{-1}), equilibrium rate constant of pseudo-second-order (g mg^{-1} min^{-1}) and intraparticle diffusion rate constant (mg g^{-1} $min^{-0.5}$), respectively.

2.7. Adsorption isotherms

Adsorption isotherms were determined at a constant room temperature of around 20°C. Different known quantities of GAC were placed in glass bottles with 250.0 mL of seawater. One of the bottles was filled with seawater alone as a control. The bottles were then overhead shaken in the dark at 15 rpm for at least 48 h to reach equilibrium. DOC was then measured in samples taken from each bottle to calculate the adsorption capacity q as follows:

$$q\ (\text{mg g}^{-1}) = \frac{V(C_i - C_e)}{M} \tag{6}$$

where V is the volume of solution (L), C_i the initial DOC concentration (mg L^{-1}), C_e the equilibrium DOC concentration (mg L^{-1}) and M the mass of GAC (g).

Adsorption isotherms were then obtained by plotting q as a function of C_e. Langmuir and Freundlich models were considered to describe these isotherms. The corresponding equations are the following:

Langmuir [32] $$\frac{1}{q} = \frac{1}{q_{max}} + \frac{1}{q_{max} K_L C_e} \tag{7}$$

Freundlich [33] $$\ln(q) = m \ln(C_e) + \ln(K_F) \tag{8}$$

where q_{max} is the maximum adsorption capacity according to the Langmuir model in mg g^{-1} and K_L is the Langmuir constant in g mg^{-1}. In Eq. (8), m and K_F (L g^{-1}) are the Freundlich parameters. If $m = 1$, the isotherm is highly unfavourable.

It was decided to study the correlation between experimental points and linearized Langmuir and Freundlich isotherms by plotting $1/q$ as a function of $1/C_e$ for Langmuir and $\ln(q)$ as a function of $\ln(C_e)$ for Freundlich, according to Eqs. (7) and (8).

The correlation between the experimental data and models was evaluated thanks to the correlation factor R^2 and the normalized standard deviation Δq (%), defined as follows:

$$\Delta q\ (\%) = 100\sqrt{\sum [(q_{exp} - q_{cal})/q_{exp}]^2/(N-1)} \tag{9}$$

where N is the number of data points, and q_{exp} and q_{cal} (mg g^{-1}) are the experimental and the calculated adsorption capacity, respectively.

2.8. GAC filter operation

GAC adsorption experiments at semi-industrial scale were performed in a fixed bed, down flow, polyvinyl chloride (PVC) column according to the column set up of Fig. 2 and the parameters of Table 5. A 200-L feed tank was filled with seawater, which was

Table 4
Most common kinetic adsorption models

Refs.	Assumptions and mechanism described	Linearized equations	
Lagergren [28]	Pseudo-first-order model	$\log(q_e - q_t) = \log q_e - \frac{k_1}{2.303} t$	(2)
Ho and McKay [29]	Pseudo-second-order. Simplified model based on experimental data only	$\frac{t}{q_t} = \frac{1}{k_2 q_e^2} + \frac{1}{q_e} t$	(3)
Weber and Morris [30]	Intraparticle diffusion model (film diffusion negligible). If $C = 0$, intraparticle diffusion is the only controlling step. If not, sorption process is complex and involves more than one diffusive resistance	$q_t = k_i t^{1/2} + C$	(4)
Elovich and Zhabrova [31]	Model based on a kinetic principle assuming that the adsorption sites increase exponentially with adsorption, which implies multilayer adsorption	$q_t = \frac{1}{\beta} \ln t + \frac{\ln(\alpha\beta)}{\beta}$	(5)

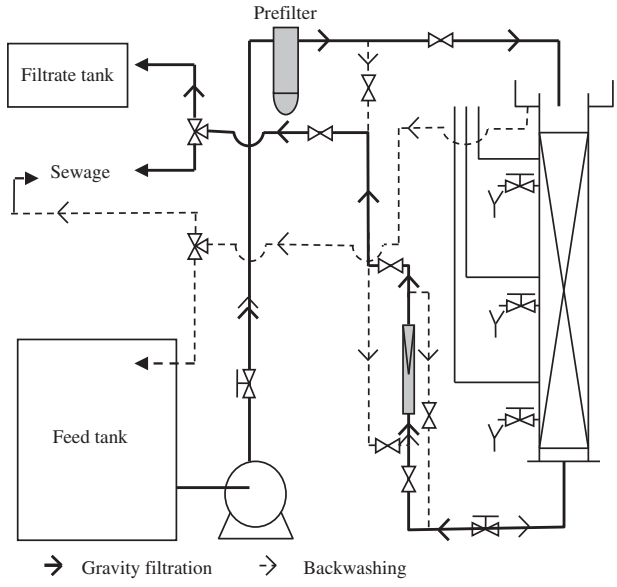

Fig. 2. Schematic diagram of GAC bed pilot plant.

Table 5
GAC adsorption column characteristics and experiment parameters

Properties	Value
Column material	PVC
GAC bed height (cm)	95
Inner column diameter (cm)	8
Average linear velocity (or hydraulic loading rate) ($m\ h^{-1}$)	3
Average empty bed contact time (min)	20
Bed porosity (from Ergun equation)	0.4
Filtration duration (h)	29

then pumped with a centrifugal pump to the head of the column where the filtration occurred under gravity. The GAC filtration was performed without recycling the filtrate. Flow rate was measured at the output of the column. A 55-µm disc filter was added between the pump and the column to protect the GAC filter from rapid fouling by large particles. The longitudinal variation of head loss was followed by means of piezometric tubes in the bed at three different heights (0, 20, and 59 cm). Variations in DOC concentrations, pH, conductivity, turbidity and $UV_{254\ nm}$ absorbance between the inlet and outlet, and at two different heights (39 cm and 78 cm) of the filtration bed were also measured during the filtration. The GAC bed was washed and backwashed with demineralized water before use.

Table 6
Value of pH_{PZC} for the different GACs

GAC	pH_{PZC} value	GAC surface charge at pH 8
A	9.7 ± 0.1	>0
B	7.8 ± 0.1	≈0
C	10.1 ± 0.1	>0
D	9.4 ± 0.1	>0
E	9.5 ± 0.1	>0
F	6.0 ± 0.1	<0

3. Comparison of the different GACs

3.1. pH of the point of zero charge

Values of pH_{PZC} obtained for the six GACs are presented in Table 6. As expected, pH_{PZC} of the physically activated GACs was basic, between 7.8 and 10.1, whereas it was acid, at 6.0, for the chemically activated GAC F. In contact with seawater at pH 8, A, C, D and E became positively charged as the water pH was below their pH_{PZC}, B was neutral and F became negatively charged. Electrostatic interactions can have an impact on DOC adsorption. Nevertheless, it has been reported that electrostatic interactions can be reduced in synthetic seawater solution ($36\ g\ L^{-1}$) as the electrical double layer of the activated carbon surface and the organic matter surface may be strongly compressed [23,34,35]. Van der Waals attractive forces could then have a greater beneficial effect on adsorption. The influence of the surface charge will be discussed later to explain DOC adsorption behaviour.

3.2. Kinetic experiments in batch mode

Fig. 3 shows the DOC removal efficiency (R_{DOC} in Eq. (1)) vs. time for each GAC until its adsorption kinetics reached equilibrium. This equilibrium was reached after 2–4 h except for GAC D, which took 10 h. As reported in Table 7, the maximum DOC removal efficiency at equilibrium increased in the order: E < C < D < B < A < F. The minimum DOC removal was 73% for GAC E and the maximum DOC removal was 86% for GAC F.

The parameters obtained with kinetic models using experimental data are listed in Table 7. Adsorption kinetics showed little or almost no (for GAC D) correlation with the Lagergren model (pseudo-first-order). In contrast, their correlation with the kinetic model of Ho and McKay, also called pseudo-second-order, was excellent (R^2 above 0.99), meaning that their kinetic adsorption behaviour was very close to a chemical reaction kinetics of second-order. The model of Weber and Morris describing an intraparticular adsorption

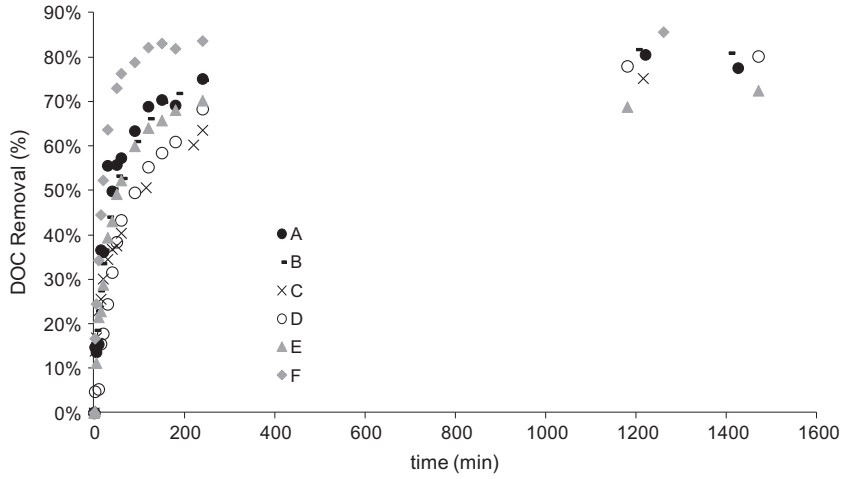

Fig. 3. DOC removal efficiency in seawater vs. time for different GACs at 7 g L^{-1}, 20°C and 15 rpm.

Table 7
Parameters of the different kinetic models for all GACs

		A	B	C	D	E	F
Maximum DOC removal efficiency at equilibrium (±3%)		81%	81%	75%	80%	73%	86%
Lagergren	R^2	0.837	0.977	0.970	0.248	0.880	0.936
Ho and McKay	q_e (mg g^{-1})	0.20	0.19	0.20	0.17	0.20	0.26
	k_2 (g mg^{-1} min^{-1})	0.24	0.22	0.28	0.36	0.08	0.44
	R^2	0.999	0.981	1.000	0.999	1.000	0.998
Weber and Morris	k_i (mg g^{-1} min^{-1})	0.02	0.01	0.01	0.02	0.01	0.04
	C (mg g^{-1})	0.02	0.05	0.040	−0.01	0.00	0.00
	R^2	0.842	0.972	0.968	0.968	0.934	0.996
Elovich and Zhabrova	R^2	0.832	0.961	0.934	0.857	0.934	0.825

process also fitted all GACs quite well (R^2 around 0.9). The C parameter of the Weber and Morris equation was very close to 0 for all kinetics, meaning that the intraparticular diffusion was almost the only limiting step of transport. A study of the effect of shaking speed and particle size should confirm this assumption. Finally, the Elovich and Zhabrova model fitted experiments quite well (R^2 around 0.9) which meant that the kinetics could involve multilayer adsorption.

Therefore, it was decided to present kinetic behaviours with DOC adsorption capacities (q in Eq. (6)) as a function of time in Fig. 4, according to Ho and McKay parameters from Table 7. For each GAC, the adsorption capacity at the end of the kinetic experiment corresponds to the equilibrium capacity q_e defined by the Ho and McKay model. However, it should be mentioned that Ho and McKay q_e may not represent a real q_e obtained from the adsorption isotherm.

With a DOC adsorption capacity of 0.26 mg g^{-1}, GAC F was clearly the most efficient at adsorbing DOC in seawater. This may have been due to its high specific surface area and high porous volume in comparison with the other GACs of this study. This will be discussed in Section 3.4. It was also the only one that was chemically activated, with the lowest pH_{PZC}, and this may have had an influence on the mechanisms of adsorption as its surface chemistry may be

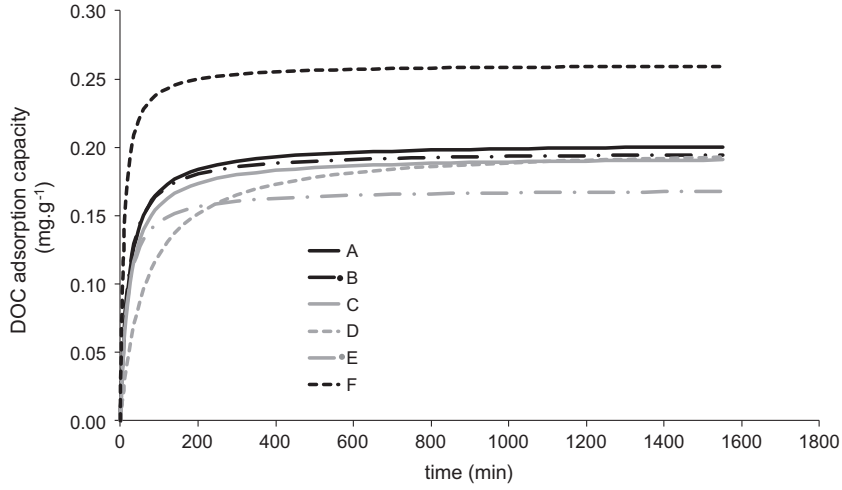

Fig. 4. DOC adsorption capacities in seawater as a function of time for different GACs obtained by Ho and McKay model from experimental data.

markedly different from that of the other GACs. Duan et al. [23] demonstrated that commercial humic acid adsorption by weakly negatively charged PAC was clearly enhanced in synthetic seawater (salinity of 36 g L^{-1}) in comparison with tap water. This was explained by some positively charged metal–humic complexes being formed with the divalent cations of seawater. Therefore, although electrostatic interactions should have a limited effect in high ionic strength solutions, experiments showed that they may have an impact for highly negatively charged GACs, such as GAC F, and the attractive electrostatic interactions did indeed seem to play an enhanced role in the DOC adsorption increase. For the other GACs, it could be assumed that the positive complexes formed by DOC and divalent cations entered into contact with a rather positive GAC surface, thanks to Van der Walls attractive forces.

GACs A, B and C showed similar behaviours, which can be explained by their similar properties. They had a rather fast adsorption rate until 100 min and, by 200 min, equilibrium had practically been reached at around 0.18 mg g^{-1}. The order of maximum DOC removal efficiency for these three GACs was of the order of their total porous volume: C < B < A.

GACs E and D were coconut-based activated carbons. GAC E showed a higher adsorption rate than GAC D at the beginning, but a lower maximal DOC adsorption capacity at equilibrium. Here, although the difference in diameters was small, it still could have played a role as GAC D had a larger particle diameter than GAC E. This could explain the longer time needed to reach equilibrium, as external transport might have been more limiting.

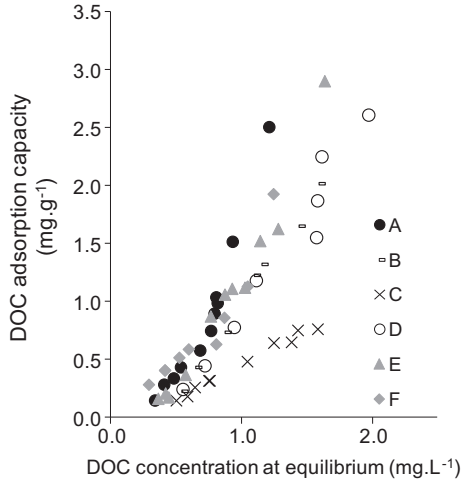

Fig. 5. Adsorption isotherms of the different GACs after at least 48 h, around 20°C, 15 rpm.

3.3. Adsorption isotherms

Fig. 5 shows the shape of the isotherms obtained for the six GACs. Experiments showed that, for the lowest value of C_e, obtained for the highest concentration in GAC, the quantity of non-adsorbable DOC could be read. The corresponding values for each GAC are listed in Table 8. Considering the uncertainty of about 3% on DOC removal, it can be considered that all GACs could adsorb about 80% of the DOC present in seawater.

The correlation with the Langmuir isotherm model was studied and gave negative maximum adsorption capacities, which had no physical meaning, and the shape of isotherms was not favourable. Consequently,

Table 8
Non-adsorbable DOC for the different GACs

	A	B	C	D	E	F
Non adsorbable DOC (±3%)	18%	23%	23%	22%	19%	17%

Table 9
Freundlich parameters obtained for the different GACs

Freundlich	A	B	C	D	E	F
Coefficient R^2	0.98	0.97	0.98	0.98	0.98	0.99
m	2.1	1.9	1.4	1.8	2.0	2.2
K_F (L g^{-1})	1.6	0.9	0.5	0.8	1.2	1.1
Δq (%)	12	13	9	12	15	9

they could not be considered as Langmuir isotherms. This was in contradiction with other published data where the GAC isotherm of DOC in seawater was found to fit the Langmuir isotherm [24]. However, in the literature, the same non-Langmuir behaviour was observed in the case of commercial humic acid adsorption by PAC in synthetic seawater [23] and it was specified that the adsorption of organic substances by activated carbon often followed the Freundlich model.

As shown in Table 9, all isotherms fitted the Freundlich model well (R^2 between 0.97 and 0.99). The parameter m was higher than 1 in all cases, confirming that isotherms were unfavourable. The Freundlich constant K_F of Eq. (8) was between 0.5 L g^{-1}, for GAC C and 1.6 L g^{-1}, for GAC A. GAC C had the lowest adsorption capacity (lowest K_F), but the least unfavourable isotherm (m closest to 1). Finally, normalized standard deviation between experimental data and data calculated with the Freundlich model was between 9 and 15%, which is acceptable.

Fig. 6 represents theoretical isotherms obtained by the Freundlich model from experimental data according to the parameters of Table 9. All GACs showed quite similar behaviour except for GAC C, for which DOC adsorption capacity was very low, probably because of its very low microporous volume in comparison to other GACs.

3.4. Effect of pore volume and specific surface area on DOC adsorption

Adsorption of DOC may be influenced by a range of factors including available pore volume and surface area. Fig. 7 illustrates this effect. Here, the adsorption isotherms obtained in Fig. 6 were replotted in terms of the mass of DOC adsorbed (a) per cm^2 of available

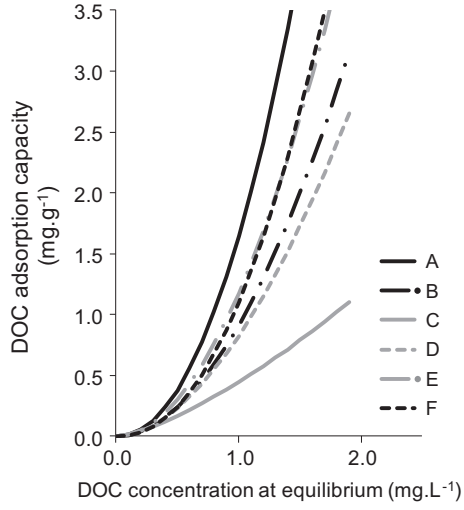

Fig. 6. Adsorption isotherms obtained by Freundlich model from experimental data.

surface area, calculated by dividing the adsorption capacity by the specific surface area and (b) per cm^3 of available pore volume, calculated by dividing the adsorption capacity by the sum of the micropore and mesopore volumes.

According to Fig. 7(a), the DOC adsorption capacity per unit surface area increased in the order C < D < F < E < B < A. This means that a larger fraction of available surface of GAC A was occupied and/or conditions (surface chemistry, pore size, etc.) were more favourable to DOC adsorption.

According to Fig. 7(b), the DOC adsorption capacity per unit volume increased in the order C < F < D < E < B < A. It seemed that, although GAC F had a better global adsorption capacity in mg g^{-1} than other GACs, its adsorption capacity per unit pore volume was lower than that of most of the other GACs, showing that a larger part of the available volume was not filled in this case. GAC A had the best DOC adsorption capacity per unit pore volume, which meant that a larger fraction of the available volume was occupied and/or conditions (surface chemistry, pore size, etc.) were more favourable to DOC adsorption.

These results showed that the high DOC adsorption performance observed previously for GAC A

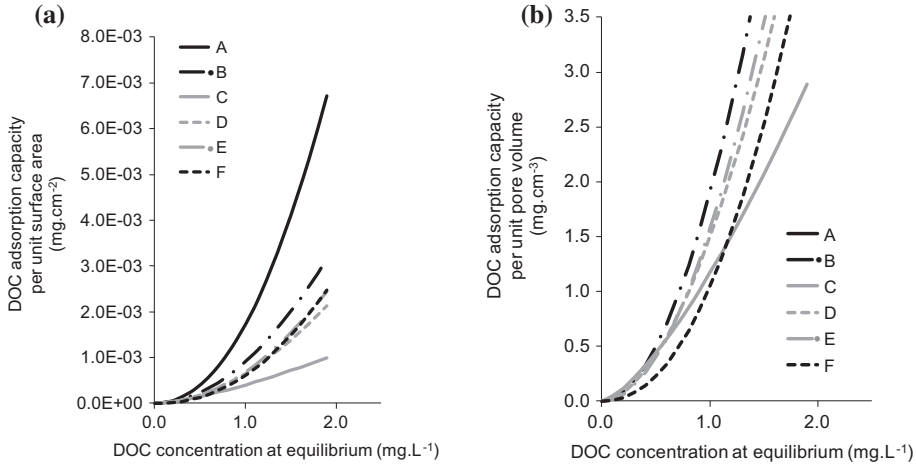

Fig. 7. DOC adsorption capacity per (a) unit surface area or (b) unit pore volume vs. equilibrium concentration for the different GACs.

could be mainly explained by the pore volume and the specific surface area (most of the available volume and surface were occupied). However, the high performance of GAC F could not be explained solely by its high available volume and surface area, but rather by its surface chemistry which may have enabled electrostatic interactions favourable to the adsorption of DOC in seawater, as previously discussed in Section 3.2.

3.5. Selection of the best GAC for filtration application

According to the previous results, GAC F proved to have the best adsorption kinetics and best adsorption capacities, with a maximum DOC adsorption capacity reaching 0.26 mg g^{-1}after only 100 min during the kinetic experiment and a non-adsorbable DOC of only 17%.

Nevertheless, with the use of this chemically activated GAC, the pH of water after each experiment mentioned above was often below 3, which is too acid. GAC is intended to be used as a pretreatment step before UF and RO. Even though acid injection is often performed before RO to prevent calcium carbonate scaling, there is a trend towards replacing this technique by the use of antiscalants [36] as acidic surface groups corrode materials and reduce the pH of the final RO permeate. Moreover, the effect of the release of acidic surface groups on UF membranes is not known. They might affect membrane lifetime, fouling and selectivity. Thus, for the rest of the study, a physically activated GAC was preferred in order to avoid the release of acidic surface groups into the water.

The GAC presenting the next best adsorption behaviour was GAC A, with a maximum adsorption capacity of 0.20 mg g^{-1} during the kinetic experiment and a non-adsorbable DOC of only 18%. In addition, GAC A had the best adsorption capacities both per unit pore volume and per unit surface area. Therefore, GAC A was chosen for the rest of the study.

4. Evaluation of the performance of a semi-industrial scale fixed bed with the selected GAC: impact on water quality

GAC filtration was performed at pilot scale to confirm the interest of GAC adsorption to reduce DOC concentration in seawater. This section characterizes the impact of GAC A bed filtration on the quality of the treated water.

4.1. Organics removal rate

Fig. 8(a) represents the DOC concentration in the GAC bed feed, filtrate and at two different heights of the bed. A 2-h stabilization step was observed for the GAC bed behaviour. Table 10 presents the main quality parameters of seawater before and after GAC filtration. The feed seawater parameters are those of the sample used for this experiment only. The filtrate values are an average calculated on the last 120 min of the experiment only. About 700 L of seawater was filtrated through the GAC bed without reaching saturation of the GAC. In the filtrate, the DOC concentration reached a value of around 0.55 mg L^{-1} which represented a DOC removal of about 70%. Other studies have reported similar rates with PAC [8,10,11] or GAC after biological growth within the bed [24]. The same behaviour was observed for the absorbance at

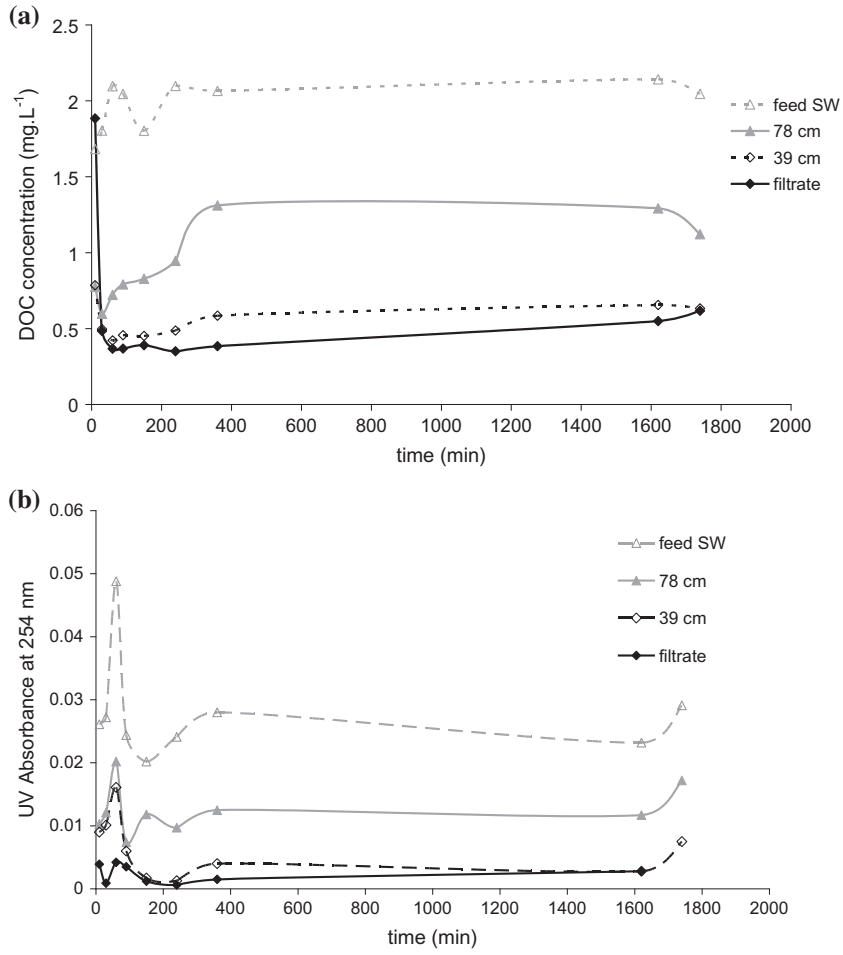

Fig. 8. (a) DOC concentration and (b) UV absorbance at 254 nm as a function of time in the GAC bed at different heights.

Table 10
Main quality parameters before and after GAC filtration (filtrate taken in the last 120 min)

Type of water	DOC (mg L^{-1})	$UV_{254\ nm}$ abs	cTEP (mg L^{-1})	Turbidity (NTU)	pH	Conductivity (mS cm^{-1})
Feed seawater	2.0 ± 0.1	0.033 ± 0.002	0.072	1.2 ± 0.1	8.2 ± 0.1	56.5 ± 0.3
Filtrate	0.55 ± 0.03	0.008 ± 0.002	0.006	0.3 ± 0.1	8.4 ± 0.1	57.6 ± 0.3
Removal rate (%)	73	76	92	75		

254 nm as presented in Fig. 8(b), meaning that, among DOC, humic acid-like substances are particularly removed. A very important result is that the measurement of cTEP, the fraction of biopolymers known to be strongly involved in membrane biofouling, showed that 92% was removed by GAC filtration.

4.2. Impact on pH and conductivity

As shown in Table 10, the conductivity in the filtrate was almost the same as that at the input: the filter did not alter the ionic composition of seawater. In the filtrate, the pH was slightly higher due to the basicity of GAC.

4.3. Retention of particles and its impact on GAC fouling

As also shown in Table 10, the turbidity in the filtrate was stable at around 0.3 NTU, representing a removal rate of at least 75%, which can be attributed to both the GAC and the prefilter. The GAC bed was not fouled after 28 h of filtration as shown by the

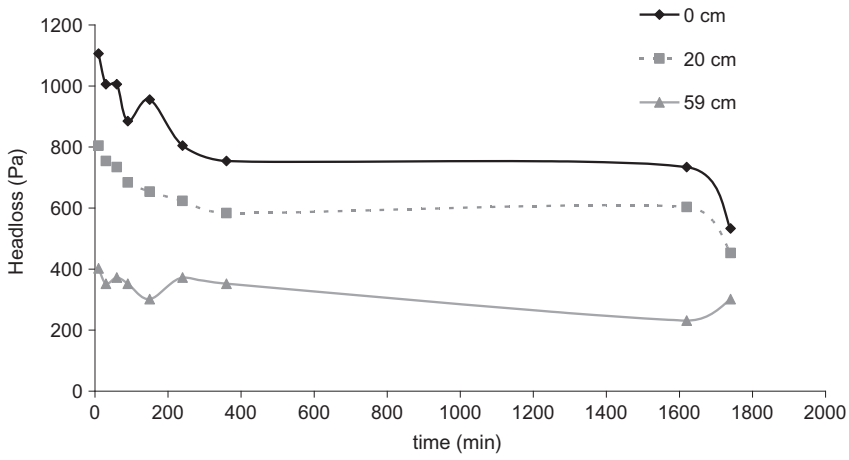

Fig. 9. Head loss in the GAC bed.

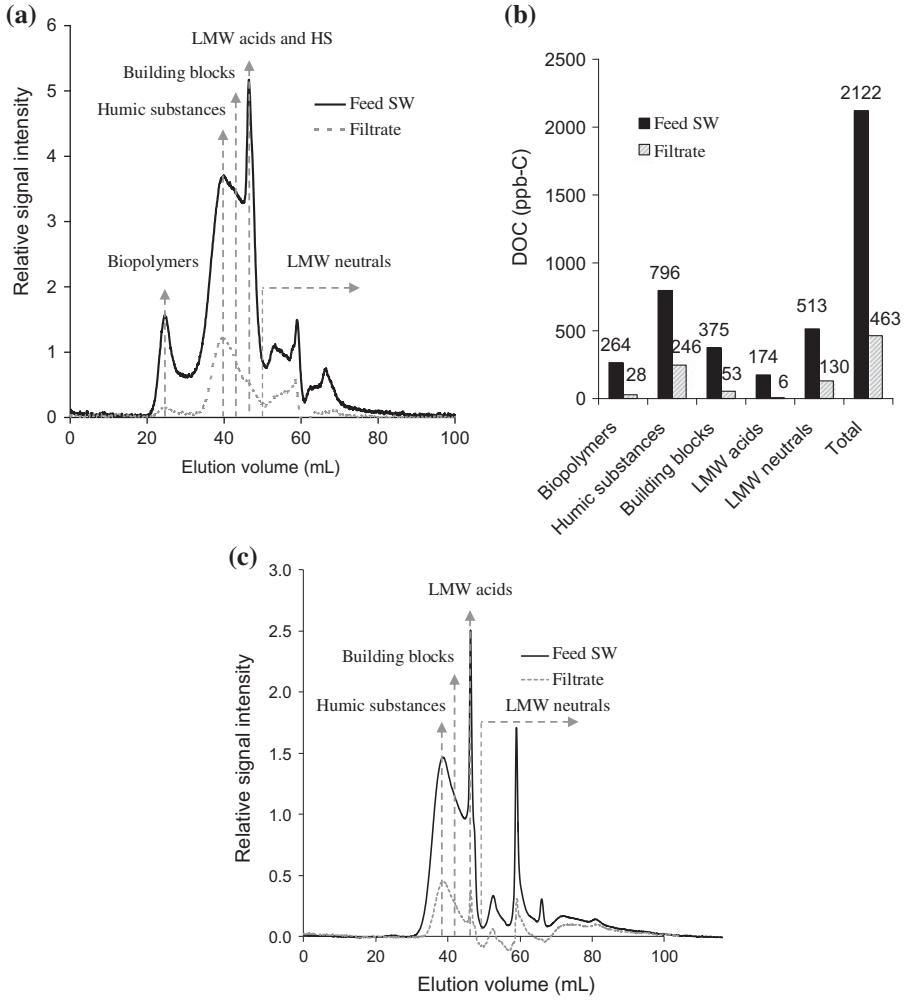

Fig. 10. (a)LC-OCD analysis chromatogram, (b) DOC fraction proportions and (c) LC-UVD analysis chromatogram comparison between feed seawater and GAC filtrate taken in the last 120 min.

constant head loss represented in Fig. 9. So, it can be supposed that the prefilter was preferentially responsible for the removal of turbidity and that the retention of particles by the GAC did not affect its permeability.

The GAC bed filtration with GAC A proved to be efficient to remove DOC from seawater, and particularly humic acid-like substances and cTEP, during the period of filtration.

4.4. GAC filtration impact on DOC fractionation

Finally, the LC-OCD chromatograms of feed seawater and filtrate are presented in Fig. 10(a) and the proportion of different organic fractions in feed seawater and filtrate in Fig. 10(b). This analysis allows an understanding of which kind of DOC molecules were better removed by the GAC bed. Fig. 10(b) shows that 13% of DOC in feed seawater was in the form of biopolymers, 37% was humic substances, 18% was building blocks, 8% was LMW acids and 24% was LMW neutrals. This distribution is similar to the one obtained for another, Mediterranean seawater [25] where the distributions were 6, 33, 18, 5 and 38%, respectively. However, the total DOC concentration in that seawater was lower (1.1 mg L^{-1}) than that in the seawater used in this work.

Fig. 10 also reveals that, in the present study, the seawater was highly concentrated in biopolymers and humic substances and this was quite uncommon (compared to standard seawater). This high concentration may be brought by terrestrial water as the seawater was sampled in coastal channels. It was noted that there was also a high concentration of LMW compounds (more than 30% of DOC) and particularly LMW neutrals, which, precisely, had to be removed by the pretreatments in order to prevent biofouling of RO membranes.

LC-OCD demonstrated that GAC bed filtration clearly reduced all fractions of DOC in seawater: biopolymers by 89% (peak at 25 mL elution volume), humic substances by 69% (peak at 40 mL elution volume), building blocks by 86% (peak at 43 mL elution volume), LMW acids by 97% (peak at 47 mL elution volume) and LMW neutrals, which were particularly targeted in this process, by 75% (peaks after 50 mL elution volume). Note that the peak at 47 mL may also contain some humic substances, but they were subtracted on the basis of their aromaticity ratios.

Fig. 10(c) presents the LC-UVD chromatograms of feed seawater and GAC filtrate where the same peaks as those of Fig. 10(a) could be observed except for the biopolymers, where no peak appeared with the UV detector. This was expected as seawater biopolymers are mainly composed of polysaccharides and proteins, which do not absorb UV at 254 nm. Humic substances and building blocks contain numerous aromatic rings as well as LMW molecules.

To conclude this section, the GAC bed filtration with GAC A was efficient during the period of filtration and greatly removed all fractions of DOC in seawater (global reduction of 78%) and, more particularly, the targeted marine DOC fractions: cTEP and LMW neutrals, which possibly meant that the pores of GAC were accessible for all sizes of DOC. Most of the remaining molecules (53% of the remaining DOC after GAC) were classified as humic substances; that is to say, mainly humic and fulvic acids of around 1 kDa.

5. Conclusions

This work aimed to better understand the mechanisms and feasibility of marine DOC adsorption and fractionation by GAC in order to prevent biofouling in RO desalination lines pretreated by UF. Six GACs with different porous structure, surface charge and specific area were characterized in the presence of natural seawater: their adsorption isotherm and kinetics showed no significant difference in terms of DOC adsorption (Freundlich isotherms and adsorption rates around 80%). Several factors have been shown to influence DOC adsorption in seawater, such as surface chemistry of the GAC, micro and mesoporous volume, surface area and particle size. It was demonstrated that GAC F and GAC A presented the best adsorption capacities in kinetics experiments with 0.26 and 0.20 mg DOC g^{-1}, respectively. These behaviours were explained by the attractive electrostatic interactions between GAC F surface chemistry and DOC and by the highest volume of pores and surface area occupied by DOC for GAC A. However, GAC F released too many acidic groups into the seawater and the possible effect of this acidification needs to be avoided in the desalination lines. Therefore, for part of the present study, GAC A was selected for operation in the semi-industrial GAC bed filtration of prefiltered seawater.

GAC filtration on a 95-cm high bed fed at 3 m h^{-1} enabled more than 70% of the DOC in seawater to be removed. Moreover, LC-OCD analysis showed that GAC fixed bed filtration drastically reduced DOC fractions, including cTEP (by 92%) and LMW neutrals (by 75%), which are known to be chiefly responsible for RO biofouling. The analysis confirmed the potential of GAC A filtration as a pretreatment before SWRO desalination. The time duration (30 h) of the experiment did not allow biofiltration to occur and the pressure losses were constant, which means that deep bed particulate fouling was negligible. In longer-term experiments,

biofiltration could take place and contribute to enhanced DOC removal [11,24,37]. Combining GAC filtration with UF in a lab-scale process is foreseen to complete this work by studying the influence of GAC on UF performance in long-term experiments on site with a continuous seawater feed.

Acknowledgements

The authors would like to thank the Hyséo company (France) for its financial and technical support and the Norit (Switzerland) and Chemviron (Belgium) companies for supplying GAC samples. They are also grateful to Ligia Barna for her precious advice concerning adsorption experiments and interpretation and to Bernard Reboul for his excellent technical assistance.

List of symbols

C_e — the equilibrium DOC concentration (mg L^{-1})
C_i — initial DOC concentration (mg L^{-1})
C_t — DOC concentration at time t (mg L^{-1})
Δq — normalized standard deviation (%)
q — adsorption capacity (mg g^{-1})
q_{cal} — calculated adsorption capacity (mg g^{-1})
q_e — amount adsorbed at equilibrium (mg g^{-1})
q_{exp} — experimental adsorption capacity (mg g^{-1})
q_{max} — maximum adsorption capacity according to Langmuir model (mg g^{-1})
q_t — amount adsorbed at time t (mg g^{-1})
k_1 — pseudo-first-order rate constant (min^{-1})
k_2 — equilibrium rate constant of pseudo-second-order (g mg^{-1} min^{-1})
K_F — Freundlich parameter (L g^{-1})
k_i — intraparticle diffusion rate constant (mg g^{-1} $min^{-0,5}$)
K_L — Langmuir constant (g mg^{-1})
m — Freundlich exponent
M — mass of GAC (g)
N — number of data points
R_{DOC} — DOC removal (%)
V — volume of solution (L)

References

[1] International Desalination Association, IDA Desalination Yearbook 2014–2015 (Water Desalination Report), Media Analytics Ltd, Oxford, UK, 2014.
[2] A. Matin, Z. Khan, S.M.J. Zaidi, M.C. Boyce, Biofouling in reverse osmosis membranes for seawater desalination: Phenomena and prevention, Desalination 281 (2011) 1–16, doi: 10.1016/j.desal.2011.06.063.
[3] H.-C. Flemming, Reverse osmosis membrane biofouling, Exp. Thermal Fluid Sci. 14 (1997) 382–391, doi: 10.1016/S0894-1777(96)00140-9.
[4] T. Berman, R. Mizrahi, C.G. Dosoretz, Transparent exopolymer particles (TEP): A critical factor in aquatic biofilm initiation and fouling on filtration membranes, Desalination 276 (2011) 184–190, doi: 10.1016/j.desal.2011.03.046.
[5] L.O. Villacorte, S.A.A. Tabatabai, D.M. Anderson, G.L. Amy, J.C. Schippers, M.D. Kennedy, Seawater reverse osmosis desalination and (harmful) algal blooms, Desalination 360 (2015) 61–80, doi: 10.1016/j.desal.2015.01.007.
[6] W.J. Lau, P.S. Goh, A.F. Ismail, S.O. Lai, Ultrafiltration as a pretreatment for seawater desalination: A review, Membr. Water Treat. 5 (2014) 15–29, doi: 10.12989/mwt.2014.5.1.015.
[7] R. Benner, B. Biddanda, B. Black, M. McCarthy, Abundance, size distribution, and stable carbon and nitrogen isotopic compositions of marine organic matter isolated by tangential-flow ultrafiltration, Mar. Chem. 57 (1997) 243–263, doi: 10.1016/S0304-4203(97)00013-3.
[8] C. Tansakul, S. Laborie, C. Cabassud, Adsorption combined with ultrafiltration to remove organic matter from seawater, Water Res. 45 (2011) 6362–6370, doi: 10.1016/j.watres.2011.09.024.
[9] A. Resosudarmo, Y. Ye, P. Le-Clech, V. Chen, Analysis of UF membrane fouling mechanisms caused by organic interactions in seawater, Water Res. 47 (2013) 911–921, doi: 10.1016/j.watres.2012.11.024.
[10] C. Tansakul, S. Laborie, C. Cabassud, Study on performance of ultrafiltration membrane-based pretreatment for application to seawater reverse osmosis desalination, Water Sci. Technol. 62 (2010) 1984–1990, doi: 10.2166/wst.2010.483.
[11] S. Jeong, H. Bae, G. Naidu, D. Jeong, S. Lee, S. Vigneswaran, Bacterial community structure in a biofilter used as a pretreatment for seawater desalination, Ecol. Eng. 60 (2013) 370–381, doi: 10.1016/j.ecoleng.2013.09.005.
[12] S. Jeong, S.-J. Kim, C. Min Kim, S. Vigneswaran, T. Vinh Nguyen, H.-K. Shon, J. Kandasamy, I.S. Kim, A detailed organic matter characterization of pretreated seawater using low pressure microfiltration hybrid systems, J. Membr. Sci. 428 (2013) 290–300, doi: 10.1016/j.memsci.2012.11.019.
[13] C. Faur, A. Cougnaud, G. Dreyfus, P. Lecloirec, Modelling the breakthrough of activated carbon filters by pesticides in surface waters with static and recurrent neural networks, Chem. Eng. J. 145 (2008) 7–15, doi: 10.1016/j.cej.2008.02.015.
[14] S.-W. Nam, D.-J. Choi, S.-K. Kim, N. Her, K.-D. Zoh, Adsorption characteristics of selected hydrophilic and hydrophobic micropollutants in water using activated carbon, J. Hazard. Mater. 270 (2014) 144–152, doi: 10.1016/j.jhazmat.2014.01.037.
[15] F. Zietzschmann, J. Altmann, C. Hannemann, M. Jekel, Lab-testing, predicting, and modeling multi-stage activated carbon adsorption of organic micro-pollutants from treated wastewater, Water Res. 83 (2015) 52–60, doi: 10.1016/j.watres.2015.06.017.
[16] B. Schreiber, T. Brinkmann, V. Schmalz, E. Worch, Adsorption of dissolved organic matter onto activated carbon—The influence of temperature, absorption wavelength, and molecular size, Water Res. 39 (2005) 3449–3456, doi: 10.1016/j.watres.2005.05.050.

[17] S. Velten, D.R.U. Knappe, J. Traber, H.-P. Kaiser, U. von Gunten, M. Boller, S. Meylan, Characterization of natural organic matter adsorption in granular activated carbon adsorbers, Water Res. 45 (2011) 3951–3959, doi: 10.1016/j.watres.2011.04.047.
[18] S. Jeong, S.A. Rice, S. Vigneswaran, Long-term effect on membrane fouling in a new membrane bioreactor as a pretreatment to seawater desalination, Bioresour. Technol. 165 (2014) 60–68, doi: 10.1016/j.biortech.2014.03.098.
[19] S.A. Huber, A. Balz, M. Abert, W. Pronk, Characterisation of aquatic humic and non-humic matter with size-exclusion chromatography-organic carbon detection-organic nitrogen detection (LC-OCD-OND), Water Res. 45 (2011) 879–885, doi: 10.1016/j.watres.2010.09.023.
[20] M.D. McCarthy, J.I. Hedges, R. Benner, The chemical composition of dissolved organic matter in seawater, Chem. Geol. 107 (1993) 503–507, doi: 10.1016/0009-2541(93)90240-J.
[21] L.O. Villacorte, M.D. Kennedy, G.L. Amy, J.C. Schippers, The fate of transparent exopolymer particles (TEP) in integrated membrane systems: Removal through pre-treatment processes and deposition on reverse osmosis membranes, Water Res. 43 (2009) 5039–5052, doi: 10.1016/j.watres.2009.08.030.
[22] S. Spotte, G. Adams, The type of activated carbon determines how much dissolved organic carbon is removed from artificial seawater, Aquacult. Eng. 3 (1984) 207–220, doi: 10.1016/0144-8609(84)90015-3.
[23] J. Duan, F. Wilson, N. Graham, J.H. Tay, Adsorption of humic acid by powdered activated carbon in saline water conditions, Desalination 151 (2003) 53–66, doi: 10.1016/S0011-9164(02)00972-4.
[24] G. Naidu, S. Jeong, S. Vigneswaran, S.A. Rice, Microbial activity in biofilter used as a pretreatment for seawater desalination, Desalination 309 (2013) 254–260, doi: 10.1016/j.desal.2012.10.016.
[25] F.X. Simon, E. Rudé, J. Llorens, S. Baig, Study on the removal of biodegradable NOM from seawater using biofiltration, Desalination 316 (2013) 8–16, doi: 10.1016/j.desal.2013.01.023.
[26] M.V. Lopez-Ramon, F. Stoeckli, C. Moreno-Castilla, F. Carrasco-Marin, On the characterization of acidic and basic surface sites on carbons by various techniques, Carbon 37 (1999) 1215–1221, doi: 10.1016/S0008-6223(98)00317-0.
[27] G. Crini, P.-M. Badot, Sorption Processes and Pollution: Conventional and Non-Conventional Sorbents for Pollutant Removal from Wastewaters, Presses universitaires de Franche-Comté, Besançon, 2010, ISBN 978-2-84867-304-2.
[28] S. Lagergren, On the theory of so-called adsorption of dissolved substances, The Royal Swedish Academy of Sciences Document, Band 24 (1898) 1–13.
[29] Y. Ho, G. McKay, Pseudo-second-order model for sorption processes, Process Biochem. 34 (1999) 451–465, doi: 10.1016/S0032-9592(98)00112-5.
[30] C.I. Weber, W.J. Morris, Kinetics of adsorption on carbon from solution, J. Sanitary Eng. Div. Am. Soc. Civ. Eng. 89 (1963) 31–59.
[31] S.Y. Elovich, G.M. Zhabrova, Mechanism of the catalytic hydrogenation of ethylene on nickel. I. Kinetics of the process, J. Phys. Chem.-USSR 13 (1939) 1761–1764.
[32] I. Langmuir, The constitution and fundamental properties of solids and liquids, J. Franklin Inst. 183 (1917) 102–105, doi: 10.1016/S0016-0032(17)90938-X.
[33] H.M.F. Freundlich, Over the adsorption in solution, J. Phys. Chem. 57(1906) (1906) 385–470.
[34] G. Newcombe, M. Drikas, Adsorption of NOM onto activated carbon: Electrostatic and non-electrostatic effects, Carbon 35 (1997) 1239–1250, doi: 10.1016/S0008-6223(97)00078-X.
[35] M. Bjelopavlic, G. Newcombe, R. Hayes, Adsorption of NOM onto activated carbon: Effect of surface charge, ionic strength, and pore volume distribution, J. Colloid Interface Sci. 210 (1999) 271–280, doi: 10.1006/jcis.1998.5975.
[36] R.Y. Ning, J.P. Netwig, Complete elimination of acid injection in reverse osmosis plants, Desalination 143 (2002) 29–34, doi: 10.1016/S0011-9164(02)00218-7.
[37] T.V. Nguyen, S. Jeong, T.T.N. Pham, J. Kandasamy, S. Vigneswaran, Effect of granular activated carbon filter on the subsequent flocculation in seawater treatment, Desalination 354 (2014) 9–16, doi: 10.1016/j.desal.2014.09.025.